ELSEVIER

Colloids and Surfaces
A: Physicochemical and Engineering Aspects 113 (1996) 11–17

COLLOIDS AND SURFACES A

Chain flattening and infrared dichroism of adsorbed poly(ethylene oxide)

Erwin P. Enriquez, Steve Granick *

Department of Materials Science and Engineering, University of Illinois at Urbana-Champaign, Urbana, IL 61801, USA

Received 13 July 1995; accepted 17 November 1995

Abstract

The adsorption of poly(ethylene oxide), PEO, from dilute solutions in 1 mM aqueous NaCl to germanium at 30°C, was investigated by polarized infrared spectroscopy in attenuated total internal reflection (ATR). PEO aggregation could be prevented with careful sample preparation. After adsorption, chain anisotropy was deduced from the C–O–C stretching vibrations along the polymer backbone and found to indicate substantial backbone alignment parallel to the surface.

Keywords: Adsorption; Chain anisotropy; Infrared dichroism; Poly(ethylene oxide)

1. Introduction

Most theoretical and experimental studies of polymer adsorption consider equilibrium structures and properties of adsorbed polymer layers [1]. However, recent studies [2–4] indicate a strong dependence of various layer properties on the kinetic history of polymer adsorption. To examine these long-lived metastable states, and the underlying distribution of conformational substates, this laboratory has previously followed the evolution of average segment orientations in the adsorbed layer by *in situ* polarized infrared spectroscopy in attenuated total internal reflection (ATR) [5]. In an exchange experiment between protio and deuterio poly(methyl methacrylate) (h-PMMA and d-PMMA, respectively), the dichroism of the methyl asymmetric stretching vibrations of the initially adsorbed h-PMMA was found to indicate a high degree of orientation that was unaffected by the influx of later-arriving d-PMMA chains. However, in that study, the exact origin of the dichroism was difficult to resolve because the PMMA repeat unit possesses two methyl groups: the backbone methyl and the sidechain ester methyl group. Seeking to directly relate dichroism measurements to backbone conformations within the adsorbed layer, we now consider the simple polymer chain of poly(ethylene oxide) (PEO), where the C–O–C backbone vibrations provide a direct measure of backbone orientation.

PEO is hydrophilic and accordingly highly soluble in water. The hydrophobic methylene groups of the backbone also allow it to dissolve in weakly polar organic solvents such as chloroform and dichloromethane [6–8]. It has wide commercial use as a nonionic surfactant, drag reducing agent, lubricant, etc. [6]. The solution behavior of PEO has been widely studied [6–16]. It exhibits a complex phase diagram with an upper critical solution temperature (UCST), a lower solution critical temperature (LCST), or a closed miscibility

* Corresponding author.

PII S0927-7757(96)03519-4

loop, depending on the solvent and molecular weight of the polymer [10]. PEO is also reported to aggregate in dilute aqueous solutions [6,11,12,16]. However, recent studies of static and dynamic light scattering with high molecular weight PEO (22000 to 1×10^6) show that the polymer does not necessarily aggregate [12,13,16].

Motivated in part by desire to understand the flocculant properties of this uncharged yet water-soluble polymer, the adsorption behavior of PEO to various mineral, silica, and other substrates has been widely investigated [17–33]. On silica, there is pH dependence to the adsorbance of PEO from aqueous solution, because adsorption occurs primarily through hydrogen-bonding at the silanol sites, whose ionization state changes with pH [17,19]. However, hydrophobic interactions with the siloxane (Si–O–Si) sites in silica also occur [17]. The reported net normalized adsorption enthalpy of PEO to silica from aqueous solutions is $\chi_s \approx 1.3$, which is relatively low [31]. A similar level of χ_s is expected in the present system.

2. Experimental

2.1. Materials

The PEO samples were used as received from Tosoh Corporation. The characteristics of the samples, as reported by the company, are given in Table 1. The NaCl (Analar grade, Aldrich) was used as received.

A literature recipe involving careful solution preparation was followed to encourage complete dissolution of PEO (molecularly dispersed) [12,13]. It has been reported that aggregates of PEO in aqueous solutions may be residual, undissolved bulk PEO [34]. Results during an early phase of this study, with inadequately prepared solutions, are discussed in the Results and Discussion section.

Table 1
Characteristics of PEO samples used

$M_w \times 10^{-5}$	M_w/M_n[a]	R_g (nm)[b]
0.46	1.10	11
9.13	1.08	64

[a] M_w and M_n are the weight-averaged and number-averaged molecular weights (g mol^{-1}), respectively.
[b] R_g, the radius of gyration, was calculated based on Ref. [13].

In following this literature recipe [12,13], the PEO was first dissolved in 1 mM NaCl with gentle shaking overnight, and then the solution was warmed at 55°C for 1 h, and finally filtered through a 0.22 mm pore size cellulose acetate filter. Prior to injection into the ATR cell apparatus, the solution was allowed to equilibrate for 1 h at the adsorption temperature of the experiment (usually 30°C).

The ATR cell apparatus and cleaning protocol were as previously reported [2]. The Ge crystal was a 45° trapezoid flat plate prism. Prior to every experiment, the Ge was cleaned as follows: (1) degreased by sonication in ethyl acetate bath for 5 min, (2) rinsed with glass distilled, deionized water, (3) treated with 5% aqueous HF solution for ≈1 min, (4) rinsed with deionized water and blow-dried with N_2 gas, (5) oxygen plasma-treated for 5 min, and (6) finally cooled to room temperature under low oxygen pressure.

2.2. Data acquisition

To eliminate air bubbles trapped within the ATR cell apparatus, it was first filled with methanol (which wets and flows freely over the stainless steel cell and Buna N Nitrile O-ring assembly) and then flipped by 180°, using the former liquid outlet tubing to let out the trapped air. The methanol was rinsed off the cell entirely by passing copious amounts of deionized water (≈500 ml). The ATR spectrum of the water-filled cell, ratioed to the spectrum of the empty cell, afforded a quick and reliable check for presence of residual methanol (which shows a strong band at 1026 cm^{-1}).

The FTIR instrument was a Biorad FTS 60 equipped with a mid-IR range mercury cadmium telluride (MCT) detector. A wire-grid polarizer was placed before the ATR cell. Spectra for p- and s-polarization directions (the electric vectors parallel and perpendicular with respect to the plane of incidence, respectively) were collected at 8 cm^{-1} resolution. Continuous data collection was done

with 64 coadded scans for the first 5 min after PEO solution was introduced into the cell, 128 scans for the next 8 min, and 512 scans for the remainder of the experiment. The interferograms were later converted to single beam spectra and then ratioed to the background spectrum, taken when the cell was filled with 1 mM aqueous NaCl only.

2.3. Data analysis

To calibrate the mass adsorbed, a calibration curve was constructed by placing solutions of different concentration into the cell. The difference between the solution spectra and those taken after solvent rinse yielded the spectra from solution alone. Fig. 1 shows the resulting calibration curve. One observes that the integrated infrared intensity increased in proportion to the solution concentration, nicely following Beer's law. The conversion to surface excess (Γ, the mass adsorbed per unit area) was performed as reported previously [2,5]:

$$\Gamma(t) = k_p A_p(t) + k_s A_s(t) \quad (1)$$

Here $k = d/(2m)$, m is the slope of the calibration curve for each polarization (p or s), and d is the penetration depth of the evanescent wave (d= 0.57 μm for the water/Ge interface at 1100 cm^{-1}), and A_p and A_s are the integrated intensities owing to the adsorbed layer, after subtraction of the contribution from non-adsorbed polymer in solution, in the p- and s-polarizations, respectively.

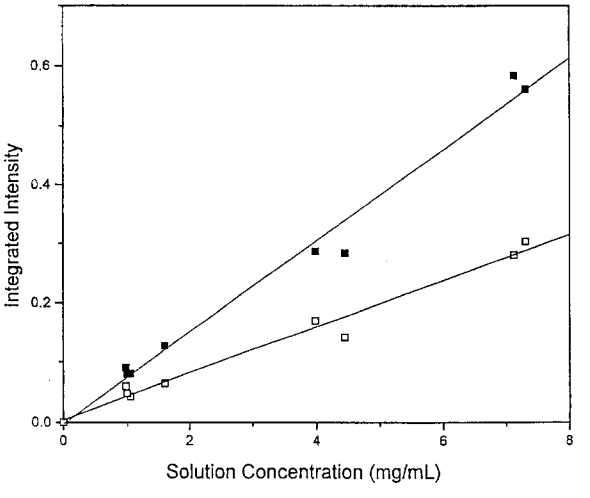

Fig. 1. Calibration curve for p- and s-polarization data (solid and open squares, respectively) of the COC band. The slopes are 0.077 and 0.039, respectively. This ratio of 2 is expected for isotropic vibrations.

3. Results and discussion

3.1. IR band assignments and quantification

Fig. 2 compares the IR spectra of a PEO free-standing film (measured in transmission) and PEO dissolved in 1 mM aqueous NaCl (measured by FTIR-ATR). Here the ATR data were obtained as follows. First the sample (M=913 000 g mol^{-1}) was allowed to adsorb from a high solution concentration (7 mg ml^{-1}), then rinsed with solution to remove the signal from non-adsorbed polymer, and finally these two signals were subtracted to give the signal of non-adsorbed polymer. One notes in Panel B of Fig. 2 that the CH_2 stretching frequency is at the edge of the intense water O–H stretch band (3300 cm^{-1}). To minimize this interference, the baseline was corrected by subtracting the H_2O band interactively. One notes that the vibrational bands of aqueous PEO are broadened and shifted compared with the bulk film spectra.

Fig. 3 illustrates how these bands were quantified. The bands of interest (CH_2 stretch region at 2900 cm^{-1} and COC at 1100 cm^{-1}) were each arbitrarily resolved into five component Gaussian peaks by a nonlinear least squares fitting procedure.

In the bulk crystalline state, PEO is known to form a 7_2 helix wherein seven repeat units comprise two turns with a period of 19.3 Å; the backbone consists of a succession of trans (CCOC), trans (COCC), and gauche (OCCO) conformations [35]. The unit cell is monoclinic, composed of four PEO helical chains [36]. The fundamental vibrational frequencies of an infinitely extended helical PEO chain (factor group $D(4p/7)$) were calculated by Yoshihara et al. [35] by normal mode coordinate analysis and compared with polarized IR spectra of oriented films. The band assignments for the spectra in Fig. 2 are given in Table 2, following the assignments by Yoshihara et al. [35].

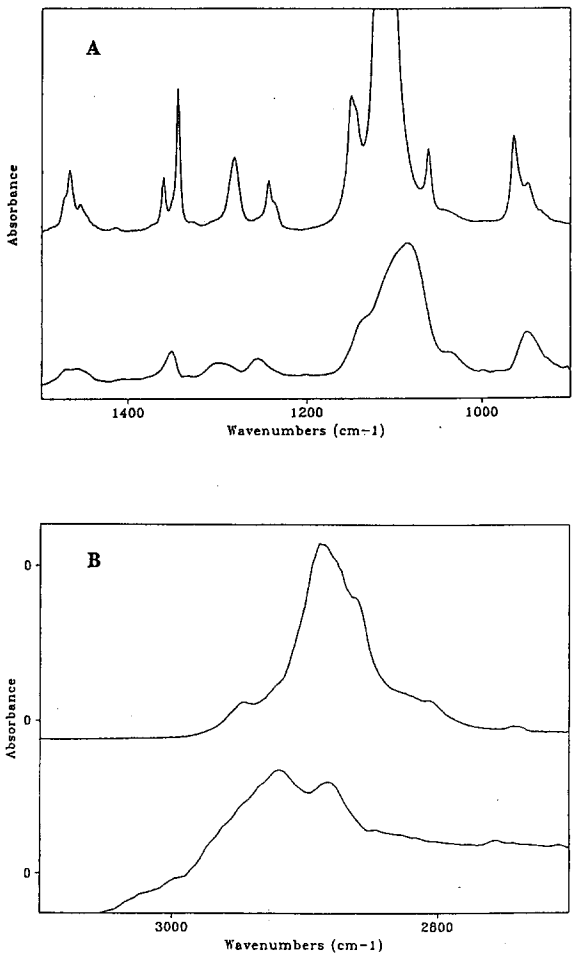

Fig. 2. Comparison of IR spectra of PEO free-standing film (transmission IR, top curve) and PEO dissolved in 1 mM aqueous NaCl (ATR-FTIR, bottom curve). (A) Low wavenumber region. (B) C–H stretch region. Band assignments are given in Table 1.

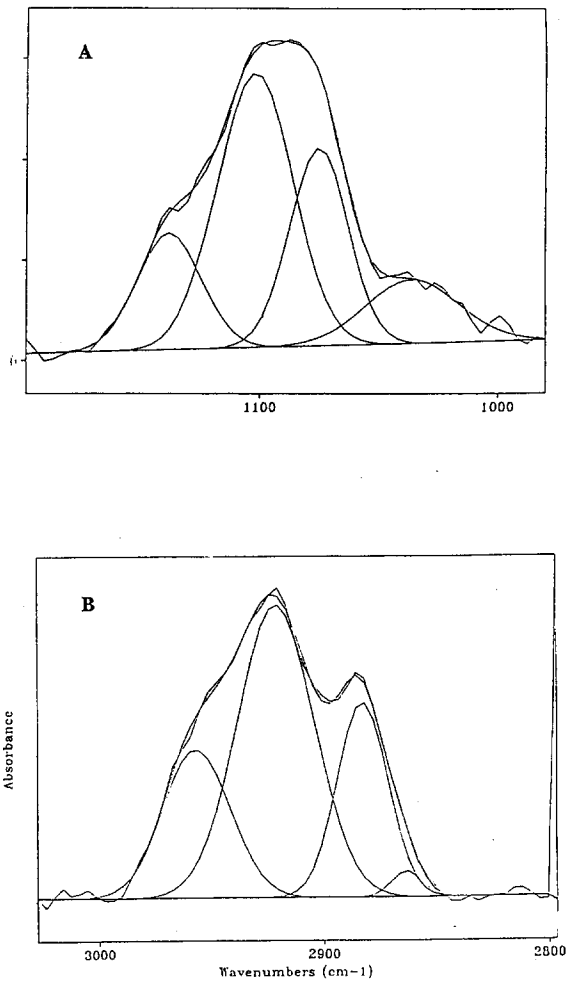

Fig. 3. Decomposition of (A) the COC band region, (B) the CH stretch band into component peaks. The CH band was baseline-corrected, after water band subtraction, to remove the weak shoulder at 2840 cm^{-1}.

In aqueous 1 mM NaCl solution at 30°C, PEO is a swollen random coil whose infrared spectrum closely matches that of PEO melt at 80°C [35,37]. For the COC stretching vibrations, significant band shifts to lower frequencies are observed for aqueous PEO (Table 2). These shifts are attributed to perturbations of the COC vibration due to hydrogen-bonding of water with the ether oxygen.

The main COC band at 1088 cm^{-1} is asymmetric and can be resolved into two component Gaussian peaks (Fig. 3A) centered at 1104 and 1078 cm^{-1}, which are tentatively assigned to the symmetric ($\nu(COC)_s$) and asymmetric C–O–C ($\nu(COC)_a$) stretching vibrations, respectively. The transition moment directions of these vibrations are reported to be preferentially parallel and perpendicular to the main chain axis, respectively [35].

The CH_2 stretching vibrations (Fig. 2B) also showed markedly different bandshapes for aqueous PEO as against the bulk PEO film. The CH_2 stretching frequencies of bulk PEO differ from those of the *n*-alkanes [35]. In contrast, the aqueous PEO spectrum shows an enhancement of the

Table 2
PEO vibrational band assignments

Wavenumber (cm^{-1})		Band assignments[a]
PEO Film	Aqueous PEO	
	2924	ν_a (CH_2)[b]
2947 sh		
2890	2882	ν_a (CH_2)
2863 sh		ν_s (CH_2)
2808 sh		
2740 sh		
2695 sh		
1468	1474	δ $(CH_2)_a - \delta(CH_2)_s$ ⊥
1455 sh	1458	$\delta(CH_2)_a$ ∥
1360 sh	1350	$\omega(CH_2)_s + \nu(CC)$ ⊥
1344		$\omega(CH_2)_a$ ∥
1281	1292	$\tau(CH_2)_a + \tau(CH_2)_s$ ⊥
1242	1250	$\tau(CH_2)_a$ ∥
1149 sh	1134	$\nu(CC) - \nu(COC)_a$
1107	1088	$\nu(COC)_a$ ∥ $+ \xi(COC)_s$ ⊥
1061 sh	1038	$\nu(COC)_a + r(CH_2)_s$ ⊥
964		$r(CH_2)_a$
948 sh	945	$r(CH_2)_s - \nu(COC)_a$

sh, shoulder; ν, stretching; δ, bending; ω, wagging; r, rocking; τ, twisting; a, antisymmetric; s, symmetric; ∥, parallel to chain axis; ⊥, perpendicular to chain axis.
[a] Adapted from Ref. [35]. [b] From assignment for *n*-alkanes, Ref. [38].

2924 cm^{-1} peak intensity; this peak matches the ν_a CH_2 of *n*-alkanes [38], and is therefore given this assignment. A similar enhancement in the 2935 cm^{-1} band for aqueous PEO was reported by Liu and Parsons [39]. The transition moment direction for this vibration is preferentially perpendicular to the backbone CC plane [39].

3.2. Adsorption from dilute solutions

Fig. 4 shows the evolution of surface excess for two PEO samples ($M = 46\,000$ and $913\,000$) adsorbed from 1.0 mg ml^{-1} solutions in 1 mM NaCl. There was rapid saturation of the layer, reaching a (pseudo)plateau within 15 min. As expected, the sample of higher molecular weight gave the higher mass adsorbed; entropically longer loops and tails, compared with the shorter chains, were favored. This dependence of surface excess on molecular weight, as well as the order of magnitude values, agree with those reported by

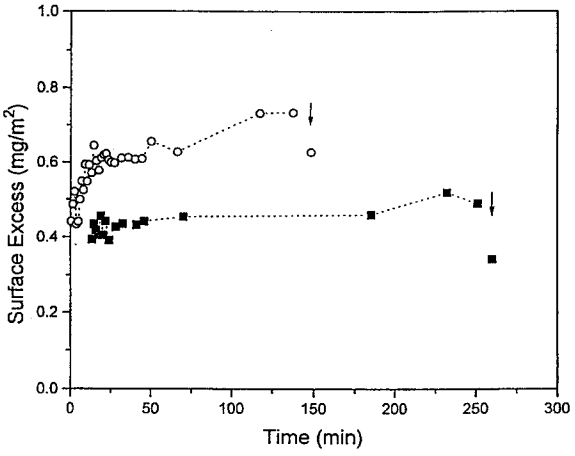

Fig. 4. Time evolution of surface excess during adsorption of PEO from 1 mg ml^{-1} solution in one mM NaCl at 30°C. Circles, $M = 913\,000$; squares, $M = 46\,000$. Measurements after solvent rinse are indicated by arrows.

Trens and Denoyel [31]. However the absolute values of the surface excess are somewhat different, presumably because of different experimental conditions, especially adsorption onto macroporous silica [31] as against Ge in our study.

For both polymers, about 0.1 mg m^{-2} adsorbed mass was washed off when the polymer solution above the layer was replaced with pure solvent. The quantity represented a larger proportion of the total for the polymer of lower molecular weight, as expected for adsorbed chains in equilibrium with solvent because of the lower overall energy of adsorption [18]. The mass adsorbed after wash is indicated, in Fig. 4, by arrows.

3.3. Aggregation of PEO

Although water is a good solvent for PEO, the literature abounds with observations of aggregates of PEO in concentrated and even dilute solutions [6,11,12,16,18]. It has been shown that careful preparation of dilute solutions of PEO in water can avoid this problem of aggregates [12,16].

In our studies we occasionally observed pronounced changes of infrared bandshape. This we attribute either to adsorption of aggregated PEO onto the Ge surface, or to aggregation of the PEO because of its high concentration at the surface.

This was particularly so during our initial studies, for which the PEO solutions were prepared neither warmed nor filtered. In this case, residual aggregates (presumably either microgels or spherulites dispersed in solution) occasionally adsorbed onto the Ge, resulting in abrupt changes of the IR bandshape to one resembling that of bulk, crystalline PEO. In fact, Polik and Burchard [11] reported the existence of dispersed aggregates with diameter $\approx$0.12–0.24 mm for unfiltered aqueous solution. In this case, passing the solution through a 0.22 mm filter, as did Devanand and Selser [12], could remove these aggregates. Warming the solution to near the melting temperature of PEO also facilitated complete dissolution of the polymer [34].

3.4. Average segment orientations

The dichroic ratio was calculated as:

$$D = A_z/A_x = A_z/A_y = (\alpha/\gamma)\,(A_p/A_s) - (\beta/\alpha) \qquad (2)$$

where the x, y, and z coordinates are as described above, and the α, β, and γ coefficients are the Fluornoy and Schaffers coefficients [40]. Here it is assumed, as we have done previously [5], that $A_x = A_y$, i.e. that there was no preferred orientation in the plane of the surface.

Dichroic ratios of the COC band were calculated from the sum of the symmetric and asymmetric vibrations. This gave significantly less scatter in data than either one separately. In principle this could have complicated interpretation of the actual backbone conformation, although this composite band is dominated by the strong asymmetric stretching vibration of COC, but in practice simply appeared to lessen the scatter without changing the trends. Dichroic ratios of the CH_2 vibration were also calculated from the two high frequency components (2924 ± 2 and $2960 \pm 3\ cm^{-1}$) of the band shown in Fig. 2B, but are not shown here owing to an unacceptable degree of scatter. We speculate that the scatter arose from the difficulty of separating the ν_a CH_2 stretch from other carbon–hydrogen vibrations.

The dichroic ratios of the COC stretching vibrations are plotted against elapsed time, in Fig. 5, for the PEO sample of highest molecular weight (913 000). Significant parallel dichroism appeared in the COC band, implying a net average parallel orientation of the PEO backbone.

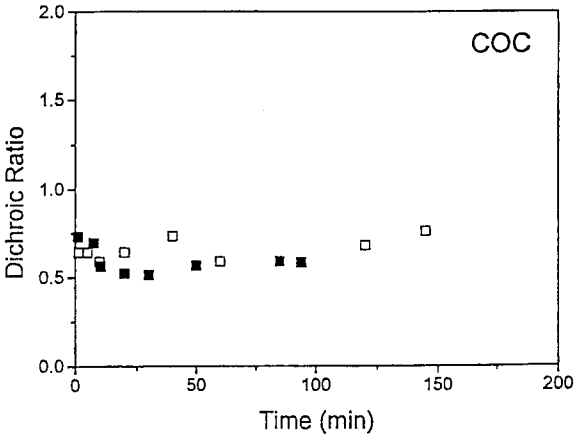

Fig. 5. Dichroic ratio, A_z/A_x, for the COC vibrations of PEO of $M = 913\,000$ adsorbed from 1.0 mg ml^{-1} solution concentration (open squares) and from 4.0 mg ml^{-1} solution concentration (filled squares). Efforts to quantify the dichroic ratio in the C–H stretch region were unsuccessful owing to scatter of the data.

Acknowledgements

We are grateful to Svetlana Sukhishvili, Iwao Soga, Hildegard Schneider, and Ali Dhinojwala for help and discussions. Support was provided through the National Science Foundation (Polymers Program), Grant NSF-DMR-91-01509.

References

[1] G.J. Fleer, M.A. Cohen Stuart, J.M.H.M. Scheutjens, T. Cosgrove and B. Vincent, Polymers at Interfaces, Chapman and Hall, New York, 1993.
[2] (a) P. Frantz and S. Granick, Macromolecules, 27 (1994) 2553: (b) H.M. Schneider, S. Granick and S. Smith, Macromolecules, 27 (1994) 4714; 4721.
[3] H.E. Johnson and S. Granick, Science, 255 (1992) 966.
[4] E. Pefferkorn, A. Haouam and R. Varoqui, Macromolecules, 21 (1988) 2111.
[5] P. Frantz and S. Granick, Macromolecules, 28 (1995) 6915.
[6] F.E. Bailey and J.V. Koleske (Eds.), Alkylene Oxides and

Their Polymers, Marcel Dekker, New York, 1991, and references cited therein.
[7] D.H. Napper, J. Colloid Interface Sci., 33 (1970) 384.
[8] E.A. Boucher and P.M. Hines, J. Polym. Sci., 16 (1978) 501.
[9] R. Kjellander and E. Florin, J. Chem. Soc. Faraday Trans. 1, 77 (1981) 2053.
[10] Y. Kambe and C. Honda, Polym. Commun., 25 (1984) 154.
[11] W.F. Polik and W. Burchard, Macromolecules, 16 (1983) 978.
[12] K. Devanand and J.C. Selser, Nature, 343 (1990) 739.
[13] K. Devanand and J.C. Selser, Macromolecules, 24 (1991) 5943.
[14] D.M. Woodley, C. Dam, H. Lam, M. LeCave, K. Devanand and J.C. Selser, Macromolecules, 25 (1992) 5283.
[15] R.L. Cook, H.E. King, Jr., and D.G. Peiffer, Phys. Rev. Lett., 69 (1992) 3072.
[16] S. Kinugasa, H. Nakahara, N. Fudagawa and Y. Koga, Macromolecules, 27 (1994) 6889.
[17] J. Rubio and J.A. Kitchener, J. Colloid Interface Sci., 57 (1976) 132.
[18] J.-F. Joanny and A.N. Semenov, Macromolecules, in press.
[19] E. Kokufuta, S. Fujii, Y. Hirai and I. Nakamura, Polymer, 23 (1982) 452.
[20] H. Hommel, A.P. Legrand, P. Tougne, H. Balard and E. Papirer, Macromolecules, 17 (1984) 1578.
[21] M. Kawaguchi, M. Mikura and A. Takahashi, Macromolecules, 17 (1984) 2063.
[22] J. Klein and P.F. Luckham, Macromolecules, 17 (1984) 1041.
[23] E. Killman, H. Maier, P. Kaniut and N. Gütling, Colloids Surfaces, 15 (1985) 261.
[24] M. Kawaguchi, A. Sakai and A. Takahashi, Macromolecules, 19 (1986) 2952.
[25] J. Klein and P.F. Luckham, Macromolecules, 19 (1986) 2007.
[26] M. Kawaguchi, T. Hada and A. Takahashi, Macromolecules, 22 (1989) 4045.
[27] M.A. Cohen Stuart and H. Tamai, Langmuir, 4 (1988) 1184.
[28] R. Denoyel and J. Rouquerol, J. Colloid Interface Sci., 143 (1991) 555.
[29] F. Lafuma, K. Wong and B. Cabane, J. Colloid Interface Sci., 143 (1991) 9.
[30] B.M. Moudgil, S. Behl and N.S. Kulkarni, J. Colloid Interface Sci., 148 (1992) 337.
[31] R. Trens and R. Denoyel, Langmuir, 9 (1993) 519.
[32] J.-S. Hsiao, A.R. Eckert and S.E. Webber, J. Phys. Chem., 98 (1994) 12032.
[33] A.R. Eckert, J.-S. Hsiao and S.E. Webber, J. Phys. Chem., 98 (1994) 12035.
[34] D. Boils and M.L. Hair, J. Colloid Interface Sci., 157 (1993) 19.
[35] T. Yoshihara, H. Tadokoro and S. Murahashi, J. Chem. Phys., 41 (1964) 2902.
[36] Y. Takahashi and H. Tadokoro, Macromolecules, 6 (1973) 673.
[37] W.H.T. Davison, J. Chem. Soc., (1955) 3270.
[38] R.G. Snyder, S.L. Hsu and S. Krimm, Spectrochim. Acta Part A, 34 (1978) 395.
[39] K.-J. Liu and J.L. Parsons, Macromolecules, 2 (1969) 529.
[40] P.A. Flournoy and W.J. Schaffers, Spectrochim. Acta, 22 (1966) 5.